Combined emulsifying capacity of polysaccharide particles of different size and shape

María Matos[a,b*], Ali Marefati[b], Romain Bordes[c*], Gemma Gutiérrez[a], Marilyn Rayner[b]

[a]Department of Chemical and Environmental Engineering, University of Oviedo, Julián Clavería 8, 33006 Oviedo, Spain

[b]Department of Food Technology, Engineering, and Nutrition, Lund University, P.O. Box 124, SE 221 00 Lund, Sweden

[c]Department of Chemistry and Chemical Engineering, Applied Chemistry, Chalmers University of Technology, SE 412 58 Göteborg, Sweden

*Corresponding authors

Maria Matos, matosmaria@uniovi.es, Tel: +34 985 103665

Romain Bordes, bordes@chalmers.se, Tel: +46 31 772 29 76

Abstract

The aim of this study is to understand mixed systems of two types of particles with different size and shape, quinoa starch granules (NQ) and cellulose nanocrystals (CNC), to stabilize oil-in-water (O/W) emulsions. This study considers the extent of Pickering stabilization with respect to which particle type dominates at droplet interfaces and how stability is affected by the addition of one particle type to already formed emulsions, or combining both, simultaneously.

Results demonstrate that the order of addition has an influence allowing to predominantly have NQ particles at the interface when both types are added simultaneously. However when CNC is added first, both types are responsible for emulsion stabilization leading to a system with an intermediate droplet size yet with a higher stability compared to single particle formulations. A dual stabilization mechanism is observed, large particles prevent coalescence and small particles regulate the curvature of the interface and govern the droplet size.

Keywords

29 Pickering emulsions, native quinoa starch (NQ), cellulose nanocrystal (CNC), size, shape,
30 stability.

31

1. Introduction

With the increasing use of pharmaceuticals, personal care products and cosmetics, there has also arisen a general awareness related to use of excipients. Many of these products are formulations based on emulsions, since the active or cosmetic substances to be transferred to the skin can be incorporated into one or more of the emulsion phases. Emulsion stabilization is often achieved through the addition of amphiphilic molecules such as small molecular weight surfactants (e.g. monoglycerides, polysorbates) which act by decreasing the interfacial tension between the phases, increase the steric hindrances and/or electrostatic repulsion between the droplets, and thereby increase the stability of the emulsion, by reducing the rate of droplet coalescence. However, one major drawback in the use of surfactants in topical formulations is that it may cause skin irritation (Welss, Basketter, & Schröder, 2004).

Pickering emulsions provide an interesting alternative to surfactant stabilised emulsions for topical applications (Justyna Frelichowska, Bolzinger, Pelletier, Valour, & Chevalier, 2009; J. Frelichowska, Bolzinger, Pelletier, Valour, & Chevalier, 2014; Marku, Wahlgren, Rayner, Sjöö, & Timgren, 2012). Particle stabilized emulsions were originally observed independently by Ramsden (Ramsden, 1903) and Pickering (Pickering, 1907). However, it was only recently that particle properties such as shape and size have been taken into account when considering the stability of Pickering emulsions, in addition to the hydrophobicity. Particles that are partially hydrophobic are better stabilizers due to their partial oil and water wettability. This allows the spontaneous accumulation of particles at the oil-water interface preventing droplet coalescence by volume exclusion and steric hindrances (Aveyard, Binks, & Clint, 2003) i.e. the particles prevent oil-water interfaces of oil droplets from coming in to direct physical contact. Thus, if particles have optimal wetting conditions (i.e. not too close to zero or 180°) and are above a certain size (approximately 10 nm) their adsorption at the oil water interface is effectively irreversible as the desorption energy per particle is several thousand kT (Aveyard et al., 2003). This strong adsorption also explains their stability (even at large droplet sizes) over extended periods of time (Rayner, Timgren, Sjöö, & Dejmek, 2012; Timgren, Rayner, Sjöö, & Dejmek, 2011).

The size and nature of particles used for Pickering emulsions varies from nanometer to micron-sized, and the resulting emulsion droplet size usually decreases with decreased

particle size, but only as long as other properties, i.e. particle wettability, shape, and concentration are the same. The particles that will primarily be used in this work are native starch granules isolated from quinoa (NQ) and cellulose nanocrystals (CNC). Both are polysaccharide-based and rather hydrophilic as they have not been modified, but with very different size and shape.

Quinoa starch granules are polygonal shaped, with a narrow size distribution ranging from 0.5 to 3 µm in diameter. Quinoa starch granules have been shown useful for topical formulation as well as encapsulation of hydrophilic and hydrophobic bioactive compound for pharmaceutical and food purposes (Marefati, Bertrand, Sjöö, Dejmek, & Rayner, 2016; Marefati, Sjöö, Timgren, Dejmek, & Rayner, 2015; Marku et al., 2012; María Matos, Timgren, Sjöö, Dejmek, & Rayner, 2013).

On the other hand, CNC is a material composed of nano-sized crystalline cellulose fragments with a high aspect ratio (length to width ratio) known for its high specific strength and modulus, high surface area and unique optical properties (Habibi, Lucia, & Rojas, 2010). Typical lateral dimensions are 5 to 20 nanometers and longitudinal dimension is in a wide range from tens of nanometers to several micrometers (Habibi et al., 2010). Cellulose nanocrystals are obtained by acid hydrolysis of cellulose fibers. Previous studies reported the ability of CNC to create Pickering emulsions with reasonable good stability during storage (Capron & Cathala, 2013; Cunha, Mougel, Cathala, Berglund, & Capron, 2014; Mikulcová, Bordes, & Kašpárková, 2016; Zoppe, Venditti, & Rojas, 2012), even for oils known to be difficult to emulsify, such as essential oils (Mikulcová et al., 2016).

The aim of this study is to understand mixed systems of two types of particles with large differences in size and shape to stabilize oil-in-water (O/W) emulsions. This study considers the extent of Pickering stabilization with respect to which particle type dominates at droplet interfaces and how stability is affected by addition of one of the particle types to already formed emulsions, or combining both simultaneously.

2. Materials and methods

2.1. Materials

Native starch granules were isolated from Bolivian quinoa grains, Chenopodium Quinoa, (purchased from Biofood-Biolivs AB, Sweden) according to the method described in section *2.2.1*. CNC were obtained by sulfuric acid hydrolysis of commercially available microcrystalline cellulose (Avicel PH101, FMC Biopolymer) according to procedure described in section *2.2.2*. The average length of the fiber was 170 nm with a diameter of 17 nm (Mikulcová et al., 2016). The external water phase was a 3 mM $CaCl_2$, density 1009.6 kg/m^3, at 20 °C. The oil phase was the medium-chain triglyceride oil Miglyol 812, density 945 kg/m^3 at 20 °C (Sasol GmbH, Germany).

2.2. Methods

2.2.1. Starch isolation

Quinoa grain was milled in a laboratory mill (Perten Instruments, Sweden). This whole grain quinoa flour contained seed coatings and large fibers in addition to the starch granules. To isolate the starch, a sedimentation method based on Stokes' law was adapted from a previous method (Dhital, Shrestha, & Gidley, 2010). First, the flour was dispersed in water at 30% (w/w) for 2 min using an overhead mixer (Ytron, Germany). The suspension was then transferred to a rectangular tank 78 by 56 by 43 cm and water was added to reach a final concentration of 5% (w/w) and thoroughly mixed.

The sedimentation was performed in two steps. Initially, the suspension was left to sediment for 1 h (to sediment the fraction > 10 µm) and the supernatant was transferred to another tank for a second sedimentation step, in which the suspension was left to sediment for 4 h (to sediment the fraction > 5 µm).

The sedimentation times for the two cut-off sizes were calculated by stokes' law (equation 1):

$$t = \frac{18\eta h}{g(\rho s - \rho w)d^2} \quad \text{(Eq. 1)}$$

where η is the viscosity of the water (1.003×10^{-3} Pa s), h is the sedimentation height (m), g is acceleration due to gravity (9.8 m/s2), ρs the density of impurities (1500 kg/m^3), ρw the density of water (998.23 kg/m^3) and d is the particle diameter (m) (Dhital et al., 2010).

After the second settling time, the supernatant (containing the fine starch granules) was carefully removed, and centrifuged (X- 15, Beckman coulter, USA) at 3000 g for 10 min

to make a compact pellet. The pellet was then mixed with NaOH solution (0.3% w/w) and centrifuged at 3000 g for 10 min and the protein residues were scraped off in multiple steps until the pellet was white. Thereafter, the pellet was mixed with citric acid (pH ~ 4.5) to neutralize the pH and centrifuged at 3000 g for 10 min. The pellet was then re-suspended in Milli-Q water and centrifuged for at least 2 times. Finally, the pellet was re-suspended in Milli-Q water and frozen using liquid nitrogen and freeze-dried (CD 12, Hetosicc, Denmark), where the temperature of the drying chamber and the cooling unit were 20 and -50 ºC respectively and the vacuum was 10^{-2} mbar. The dried powder was removed from freeze dryer and ground using a mortar and pestle.

2.2.2. Preparation of cellulose nanocrystals

The preparation is based on a protocol adapted from Bondeson, Mathew, and Oksman (2006), and details can be found elsewhere (Bondeson et al., 2006). In brief, 40 g of microcrystalline cellulose (Avicel PH-101 NF) was dispersed in Milli-Q water (400 ml) in a 2 L Erlenmeyer flask while stirred and cooled by an ice bath. Sulfuric acid (95-98%, w/w) was added to reach a final concentration of 64% (w/w), while holding the temperature below 20 °C. The mixture was then heated to 45 °C for 130 min, after which 4 L of deionized water was added. The solid was washed by centrifugation 3 times. The cellulose suspension was dialyzed (membrane cut-off 12000-14000 Da) for 3 weeks, with water replacement twice a day. The cellulose was then sonicated (Vibracell Sonicator, Sonics and Materials Inc., Danbury, CT) at 40% output in 3 cycles of 14 min each, to be finally ion-exchanged (Dowex Marathon MR-3 resin, H-form). The CNC suspension was finally titrated by conductivity with a NaOH solution (0.02 M). The suspension was concentrated to 2% (w/w) with a rotary evaporator.

2.2.3. Characterization of particle charge density

Charge density titration was performed with a solution of polyDADMAC (0.001 N) using a Particle Charge Detector, CAS Charge Analyzing System (AFG, Analytic GMBH). The value of 250 µEq/g and 5 µEq/g found was the average of 3 measurements for CNC and NQ respectively.

2.2.4. Preparation of Pickering emulsions stabilized with NQ or CNC particles

Emulsions with 10% (w/w) of Miglyol 812 were prepared in 7 mL volumes. The oil phase was dispersed in a continuous phase of 3 mM $CaCl_2$ solution containing varying concentrations of NQ in granular non-dissolved state, i.e. 0.05, 0.10, 0.20, 0.30, 0.40, 0.50, 0.75, 1.0, 2.0 and 4.0% (w/w). The corresponding starch-to-oil ratios were therefore 5, 10, 20, 30, 40, 50, 75, 100, 200 and 400 mg/mL. This was emulsified in glass test tubes by high shear mixing by a Heidolph Silentcrusher-M (Heidolph, Germany) with 6 mm dispersing tool at 22000 rpm for 30 s. Formulation and stirring conditions were based on previous studies.(Rayner, Timgren, et al., 2012) All the emulsions were prepared in triplicate.

For the CNC-stabilized emulsions, the continuous phase consisted of 3 mM $CaCl_2$ solution containing varying concentrations of CNC. Emulsions were prepared with the same mass particles-to-oil ratios and emulsification conditions as for the starch emulsions.

$CaCl_2$ was used in all the cases to enhance the emulsion stabilities (Cherhal, Cousin, & Capron, 2016).

2.2.5. Preparation of emulsions stabilized by a combination of NQ and CNC particles

Emulsions were stabilized by a combination of NQ and CNC with a ratio 1:1 (w/w). Emulsions were prepared at 10% oil (w/w) emulsifying the mixture under the same homogenization conditions as described in section *2.2.4*. The order of addition was investigated. For this purpose, emulsions were prepared adding both types of particles simultaneously or subsequently.

2.2.6. Emulsion characterization

2.2.6.1. Size and particle size distribution of emulsion droplets

Particle size distributions of the emulsions were measured by laser diffraction using a Malvern Particle Size Analyzer (Mastersizer 2000S, Malvern Instruments Ltd. UK). The sample was added to the flow system containing Milli-Q water and was pumped through

the optical chamber at a pump setting of 2000 rpm. A refractive index (RI) of 1.54 and 1.42 was used for the starch and CNC Pickering emulsions samples respectively while the RI of the continuous phase was set to 1.33 (water). The obscuration ranged between 10 and 20%.

2.2.6.2. Optical microscopy

Micrographs of the emulsions were obtained immediately after emulsification with a light microscope (Olympus BX50, Tokyo, Japan) with 5-100× magnifications and digital camera (DFK 41AF02, Imaging source, Germany) and processed with the software ImageJ (NIH, version 1.42m).

2.2.6.3. Scanning electron microscopy (SEM)

Starch granules, CNC particles and dried Pickering emulsions were characterized by scanning electron microscopy (SEM). Initially, the emulsion samples were freeze dried using a laboratory freeze dryer (CD 12, Hetosicc, Denmark). In order to avoid destabilization of the emulsions during freezing and freeze-drying, shea nut oil with melting point of 33 ºC (AAK, Karlshamn, Sweden) was used according to previous studies (Marefati, Rayner, Timgren, Dejmek, & Sjöö, 2013; Marefati et al., 2015). Shea nut oil was kept in a water bath of 40 ºC prior to emulsification and thereafter, the emulsification was carried out according to the method described in section *2.2.1*. The dried samples were coated with gold and examined under SEM (field emission SEM, JSM-6700F, JEOL, Japan) Operated at 5 kV with a working distance of 8 mm. Lower detection imaging mode (LEI) was used to give clear images of the sample surface. The LEI detector combines both signals of secondary and backscattered electrons during operation. CNCs were examined using a LEO Ultra 55 field emission gun (FEG) SEM (Carl Zeiss, Germany), operating at an acceleration voltage of 2–3 kV. The specimens were prepared as follow: a 20 µl 0.1% (w/v) polyethyleneimine drop was put on a clean silicon wafer. A 20µl drop 0.05% (w/w) CNC was then deposited on the surface for one minute, then flushed with nitrogen gas. Finally the specimen was sputtered with an Au layer of ca. 1-2 nm

2.2.6.4. Emulsions stability studied by static multiple light scattering (MLS)

Emulsion stability was evaluated directly after emulsification by static multiple light scattering (MLS) using a Turbiscan Lab Expert (Formulaction Co., France), which operates by sending a light beam through a cylindrical glass cell containing the sample.(M Matos, Gutiérrez, Iglesias, Coca, & Pazos, 2015) Emulsions were placed without dilution in the test cells and the transmitted and backscattered light intensity (TS and BS, respectively) were monitored as a function of time and cell height at 30 °C, with a vertical resolution of 40 µm. Emulsions were monitored by scanning the sample every minute for one hour. These profiles build up a macroscopic fingerprint of the emulsion at a given time providing useful information about changes in droplet size, appearance of creaming or a clarification processes allowing one to monitor the height of the clarification front and migration velocity of creaming oil droplets as a function of time (María Matos, Lobo, Benito, Coca, & Pazos, 2012; María Matos, Marefati, Gutiérrez, Wahlgren, & Rayner, 2016).

3. Results

For all the particles systems used in this study, O/W emulsions were formed. This is in agreement with previous reports, where only CNC or starch were used (Mikulcová et al., 2016; Rayner, Sjöö, Timgren, & Dejmek, 2012).

3.1. Size and size distribution of emulsion droplets

The emulsion droplet size as a function of starch concentration for the different particle types is plotted in Fig. 1. As expected the droplet size decreased as the amount of NQ starch increased. This is in agreement with previous observations on native quinoa starch particles stabilized emulsions (María Matos et al., 2016; Timgren et al., 2011). Full particle size distribution and data of emulsion stabilized by NQ, CNC and mixtures of CNC then NQ are provided in supplemental material Fig. S.1A-C and Table S.1. The $D_{[4,3]}$ varied from ~ 140 µm at 0.05% (w/w) to ~ 30 µm at 4% (w/w). The particle size measurements for CNC stabilized emulsions showed smaller mean droplet sizes compared to NQ stabilized emulsions. Moreover, the mean droplet size of CNC emulsions was less affected by particle concentration (from ~ 80 µm to ~ 50 µm) than

NQ over the same range of concentrations. This is in agreement with previous results for CNC (Mikulcová et al., 2016) and starch (Rayner, Sjöö, et al., 2012) particle stabilized emulsions, where smaller droplet sizes were obtained at higher particle concentration due to the fact that more particles are available to stabilize larger overall interfacial area. The size difference is not so large, however, especially considering the nano-sized character of CNC compared to starch. This seems to indicate that the larger dimension of CNC, i.e. its length, is the limiting factor to increase the curvature of the interface. Despite significantly smaller dimension when it comes to the width, CNC is more comparable to NQ starch in terms of length.

Emulsions combining the two particle types were prepared by two different approaches, either by combining the particle in the aqueous phase followed by emulsification, or in a competitive manner by forming the emulsion with a single type of particle and then adding the other type of particle. From Fig. 1, several observations can be done. First, a decrease in size can be noticed with particle concentration (in the range 0-1% w/w), irrespective of the order of addition and particle type. At low particle concentration, similar sizes to the ones obtained with NQ particles were obtained when NQ was added first or when both types of particles were added simultaneously. Similar to pure NQ formulations, at concentrations higher than 0.50% w/w, a more pronounced decrease in mean droplet sizes was observed, but not to the same extent as the pure NQ formulation. This suggests that in mixed particle formulations the NQ particles have a predominant effect on the resulting mean droplet size. The effect of NQ particles was less pronounced when CNC was added first and the resulting mean sizes were in between sizes obtained with single particle type formulations.

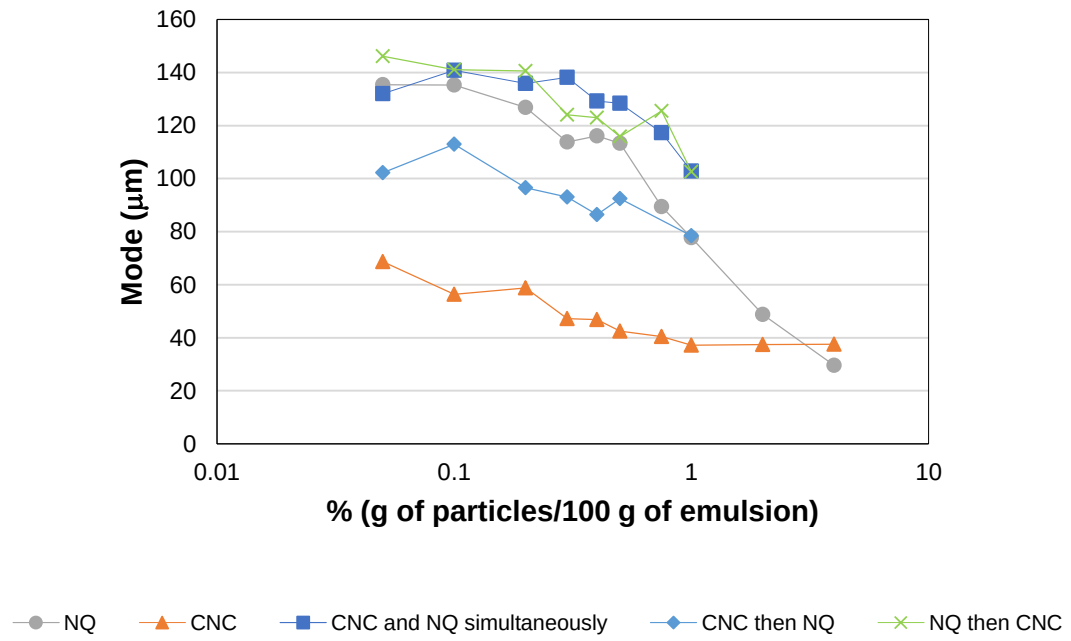

Fig. 1. Mode of Pickering emulsions with 10% (w/w) oil content prepared at different concentrations of NQ starch, CNC particles or mixtures of both prepared at different orders of addition

The cumulative droplet size distributions (Fig. 2) confirm this observation and shows that when CNC particles were added before NQ particles the resulting size of the emulsion droplets was more affected by the amount of CNC. This effect was more pronounced in the concentration range 0.05 to 0.30% (w/w) (Figs. 2A, B, C and D) since at 0.50% (w/w) all sizes are similar for emulsions prepared either with NQ particles only or with any possible combination of NQ and CNC particles regardless the order of addition (Fig. 2). Interestingly, the CNC efficiency decreases around this concentration, as the droplet size reaches a plateau (Fig. 1).

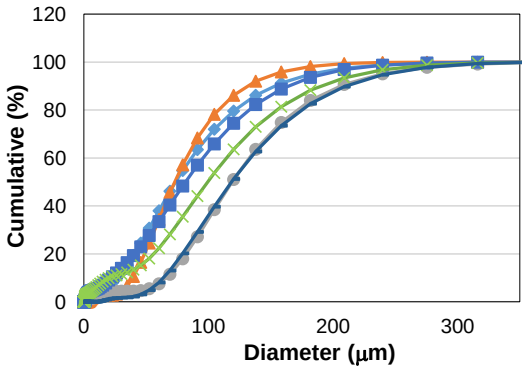

A. 0.05 % (w/w)

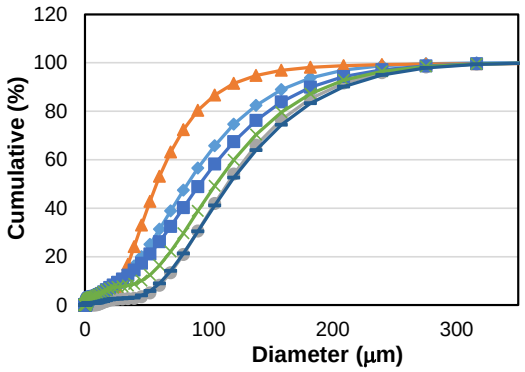

B. 0.10 % (w/w)

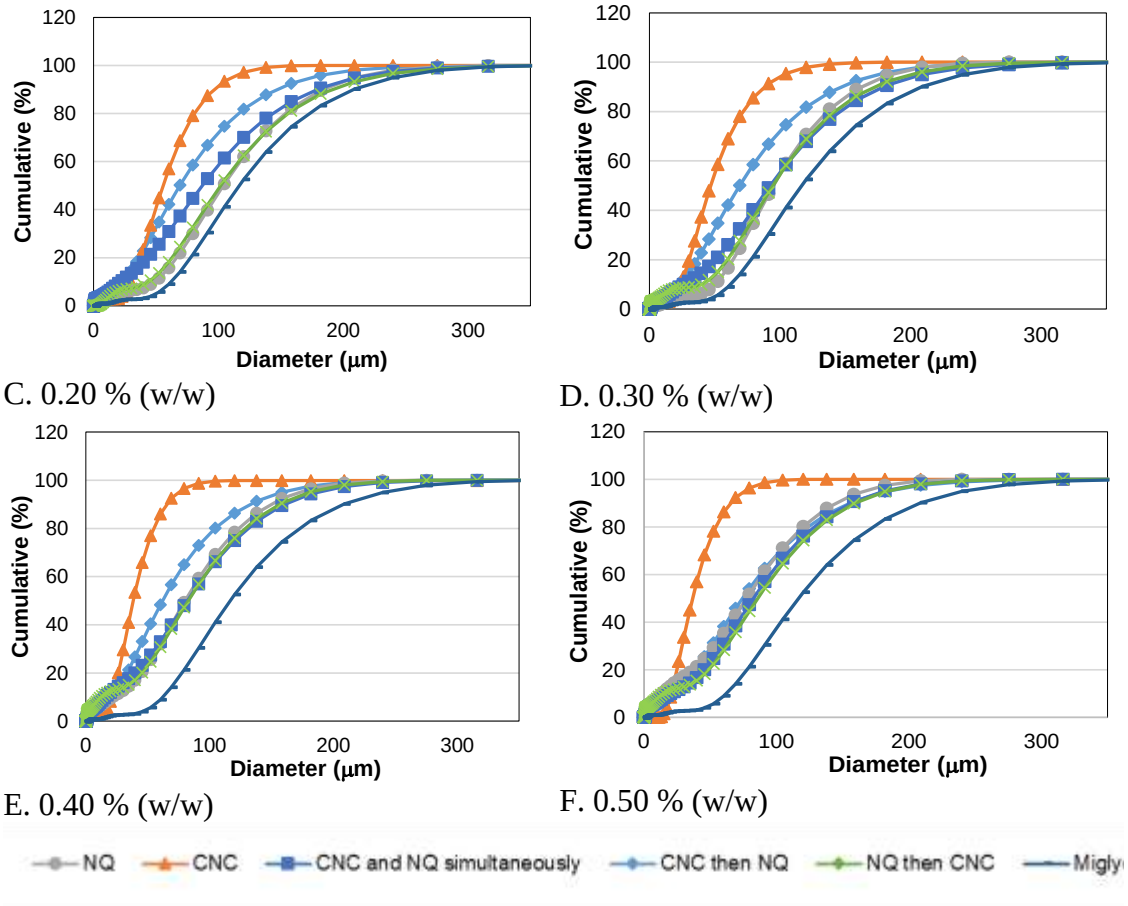

282 Fig. 2. Cumulative droplet size distributions of Pickering emulsions with 10% (w/w) oil
283 content prepared at different concentrations of NQ, CNC or mixtures of both
284 prepared with different orders of addition

285

286 *3.2. Optical microscopy*

287 Microscope images were recorded in order to qualitatively evaluate the interfacial
288 composition of the oil droplets, and are shown in Fig. 3. Thanks to its large size, especially
289 in comparison with CNC, NQ particles can be easily identified on the surface of the oil
290 droplets (Fig. 3B, E and H). In the case of emulsions stabilized with CNC particles (Fig.
291 3A, D and G) it is not possible to estimate the coverage. The mean droplet sizes are in
292 good agreement with results obtained from the laser diffraction experiments, however.
293 NQ starch granules were also distinguished around droplets surface for emulsions
294 prepared by combination of particles where CNC particles were added first and then NQ
295 particles (Fig. 3C, F and I). However, in that case the surface coverage by the NQ granules
296 seems to be lower compared to images shown in Fig. 3B, E and H. These emulsions

297 showed a resulting mean size comprised between the sizes obtained by single particle
298 type formulations.

299

300

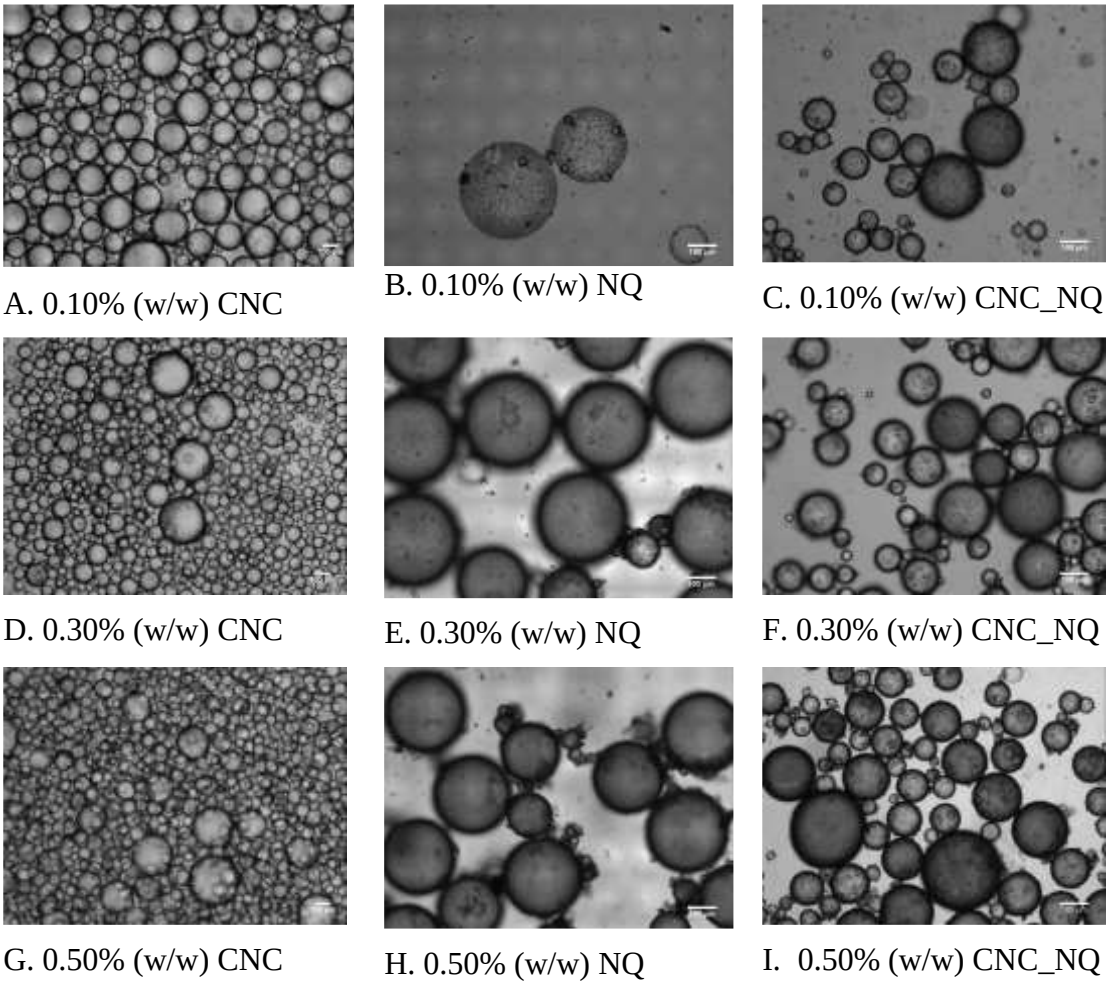

301 Fig. 3. Light microscopy images of the O/W emulsions with 10% (w/w) oil content
302 prepared at different concentrations of CNC (A, D and G), NQ (B, E and H), or
303 mixtures of both adding first CNC and then NQ (C, F and I)

304

305 *3.3. Electronic scanning microscopy (SEM)*

306 SEM images were obtained in order to know more about the morphology of the particles
307 used in this study and also the character of the resulting Pickering emulsions. Fig. 4A
308 shows the fibril nature of CNC particles after being deposited on a flat surface. It can be
309 observed in Fig. 4B that the native starch granules isolated from quinoa are unimodal and

polygonal shaped with a mean size around 1 µm. This is in good agreement with previous observations under same conditions (Marefati et al., 2016; Timgren et al., 2011).

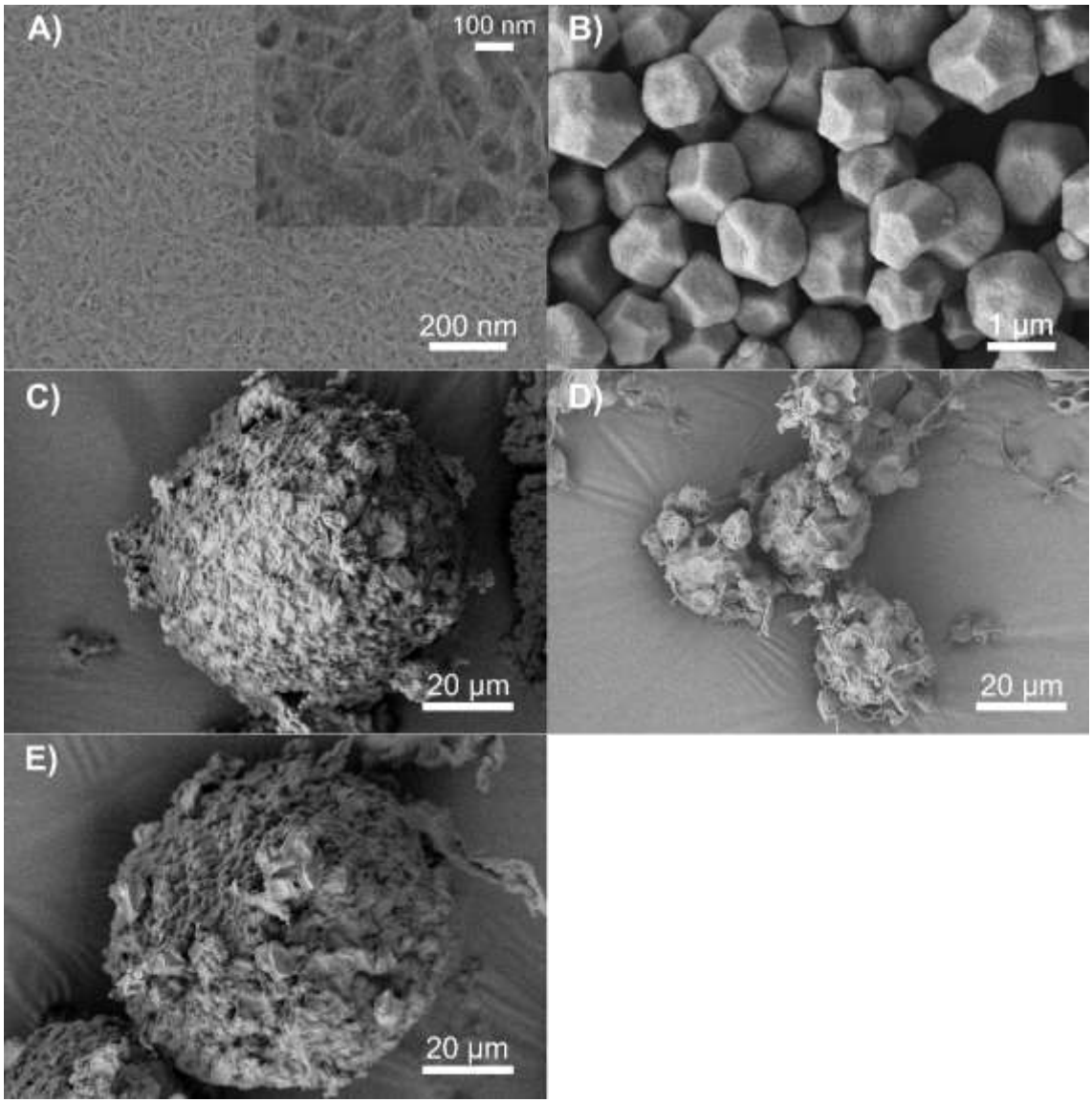

Fig. 4. SEM images of CNC (A), NQ (B), Pickering emulsions with 10% (w/w) oil content prepared using NQ (C), CNC (D) and a combination of CNC and NQ where CNC was added first (E)

Fig. 4C and 4D show the emulsion stabilized solely by NQ and CNC particles, respectively. Even though part of the surface roughness can be attributed to the freeze-drying process, as the formation of crystals can never be completely prevented, it is clear that the NQ Pickering emulsion droplets are less smooth than the CNC ones. In Fig. 4C the NQ granules can be easily identified at the droplet surface.

In the mixed particle formulations, the predominant character of NQ at the surface can be noted at the droplet surfaces, however this dominance is weaker, when CNC particles were added first (Fig. 4E). This observation confirms results obtained from the microscopy and particle size analysis.

3.4. Emulsion stability studied multiple light scattering (MLS)

Stability of the emulsions was monitored with MLS using backscattering and a stability index as mean of evaluation. The backscattering (BS) measurement is directly dependent on the particle mean diameter and on the volume fraction. The main instability phenomena observed in colloidal systems can be of different nature: particle migration (i.e. local variation of the concentration of particles which causes a local variation of the transmission or backscattering level measured at the bottom and top of the sample); particle size increase (i.e. global variation of the particle size which causes a global variation of the transmission or backscattering level measured in the middle of the sample). Therefore, BS variation in the middle part of the cell (ΔBS_{middle}) was measured for emulsions prepared at a fixed concentration of particles using either CNC, NQ or combination of both. A stability index commonly referred to as Turbiscan Stability Index (TSI) was also calculated to compare the stability of the different formulations studied. The TSI is the sum of all the variations detected in the samples in terms of size and/or concentration, and is defined by the following equation:

$$TSI = \sum_i \frac{\sum_i |scan_i - scan_{i-1}|}{H} \quad \text{(Eq. 2)}$$

A low value of TSI usually implies a stable emulsion, as it reflects minor changes in the emulsion aging (Matos et al. 2016).

The TSI results are shown in supplemental material Table S.2 together with ΔBS_{middle} for emulsions prepared containing 10% (w/w) of oil stabilized with 0.05, 0.10, 0.30 and 0.50 % (w/w) (g of particles/100 g of emulsion) using CNC, NQ starch or mixtures of both adding CNC and NQ subsequently.

Low values of TSI and ΔBS_{middle} were obtained when emulsions were stabilized with NQ or a combination of CNC and NQ particles (added sequentially), being in the range 0.485-1.366 and 1.626-2.989 respectively. Previous MLS results with Pickering emulsions showed that they kept their droplet size constant and were stable against coalescence and

other destabilization processes (María Matos et al., 2016). Higher values were obtained when the Pickering emulsions were stabilized with CNC as emulsifier leading to ΔBS_{middle} up to 4.838 and TSI values around 4.544. Moreover, higher stability against coalescence was obtained when CNC and NQ were used as stabilizers adding them subsequently compared to emulsions formulated only with CNC (see in supplemental material Fig. S.2). Also higher stability against sedimentation and creaming was obtained with these emulsions stabilized by CNC-NQ mixtures when comparing to NQ-stabilized Pickering emulsions (Fig. S.2). Therefore, these results suggest that a combination of CNC and NQ particles could enhance the stability of the resulting Pickering emulsions against destabilization phenomena.

4. Discussion

The use of emulsion stabilizing particles with different shape and size, yet consisting of material similar in nature, in a competitive manner, while benchmarking the performance of the specific particles alone, offers the possibility of evaluating the role of the particles characteristics such as size, and shape, on two major aspects of the emulsions, namely the emulsification process and the stabilization mechanism.

4.1 Emulsification processes in particle stabilized dispersions

4.1.1 Particle packing and droplet size

During the homogenization process of generating particle stabilized emulsions, the evolution of the mean drop size is governed by competition of two opposing mechanisms: drop break up and drop-drop coalescence. The rate and magnitude of these two processes determine the final drop size and a result of the type and concentration of the stabilizing particles, the volume fraction of dispersed phase and the hydrodynamic conditions inside the homogenization device. At low particle concentration, the mean drop size rapidly decreases with increasing concentration. Under these conditions drops that have been created, but do not have a sufficient amount of particles will re-coalesce. This continues until the resulting drop has enough surface coverage to prevent further coalescence events (Arditty, Whitby, Binks, Schmitt, & Leal-Calderon, 2003). This process is often referred to a limited-coalescence and the final droplet size for a given concentration and geometry

of particles can be predicted by a simple mass balance (equation 3) at the interface with the following assumptions: there is no barrier to adsorption, the transport of particles to the interface is not limiting, and the amount of un-adsorbed particles is negligible (Tcholakova, Denkov, & Lips, 2008).

$$d_{32} \approx \frac{6\phi}{(1-\phi)} \frac{\Gamma_M}{C_p} \theta^* = \frac{8\phi}{(1-\phi)} \frac{a\rho_p\varphi}{C_p} \theta^* \quad \text{(Eq. 3)}$$

Where d_{32} is the droplet diameter, ϕ is the dispersed phase fraction, Γ_M is maximum mass per m^2 of emulsifier adsorbed as a close packed monolayer at the drop interface, a is the particle radius, ρ_p, is the particle density, φ is the monolayer surface coverage of (spherical) particles $\varphi = \pi/\sqrt{12} \approx 0.901$, C_p is the mass concentration in the continuous phase, and θ^* is the minimum fraction a monolayer surface coverage required to prevent coalescence and in most cases is close to one for small, non-aggregating particles (Tcholakova et al., 2008). In equation 4a, Γ_M is given for spherical particles:

$$\Gamma_M \approx \rho_p \frac{4/3\pi a^3}{\pi a^2} \varphi \approx \rho_p \frac{4}{3} a\varphi \quad \text{(Eq. 4a)}$$

For an ellipsoidal shaped particle, such as CNC the equation becomes:

$$\Gamma_M \approx \rho_p \frac{\frac{4}{3\pi abc}}{\pi ab} \varphi \approx \rho_p \frac{4}{3} b\varphi \quad \text{(Eq. 4b)}$$

where b, and c are the lengths of the semi-major axis and semi-minor axes respectively, in the present case $b = c$.

In this work we increased the particle concentration from very low to moderate concentrations in order to see what concentration of particles no longer affects drop size, i.e. the extent of the limited coalescence regime where equation 3 could predict drop size. If we compare the predicted d_{32} droplet diameters for NQ and CNC based on their geometry and concentration used, we will find that the predicted drop diameters are much larger than the measured data for the NQ and much smaller for the CNC over the entire measurement range. This indicates that several other phenomena are taking place. In the case of the NQ, we strongly suspect $\theta^* < 1$, as full surface coverage becomes less critical for particles that have a dimension that is non-negligible compared to the curvature of the oil-water interface. However in the case of CNC, the larger than predicted droplet sizes would suggest that other phenomena, beyond simple geometry, are taking place, such as electrostatic repulsions.

The two other factors that could be affecting the final drop size are the rate of transport of particles to the oil – water interface, and any barrier to adsorption they may encounter on their way to the interface.

When observing the results from the competitive experiments and the fact that NQ particles tend to have a strong influence on droplet size, suggest that packing of spherical systems is somewhat easier, and that the presence of CNC, most likely owing to its small size, does not jam the interfacial organization of the NQ particles.

4.1.2 Effect of particle geometry on convective transport to the interface

Unlike surfactants, protein molecules, and nanoparticles < 2 nm, where Brownian motion is the main transport mechanism for overcoming adsorption barriers, the transfer of larger particles (i.e. 10s of nm) to the oil-water interface from the bulk continuous phase are governed by convective transport.(Tcholakova et al., 2008) There also appear to exist a transitional size range (2 – 23 nm) where neither Brownian diffusion nor convective transport is especially effective in enabling particle adsorption (Tcholakova et al., 2008).

One possible explanation to the differences emulsification results between the micron-sized NQ granules and the nano-sized CNC is the kinetics of their convective transport during emulsification, i.e. their size and inertia relative to the turbulent eddies created by the homogenisation device used. In this work we used a 6 mm toothed-disc disperser. In general, this type of laboratory scale high-shear homogeniser operates with a bounded turbulent-viscous flow and can achieve a power density, ε, of 10^3 to 10^8 W/m^3.

Hydrodynamically, the turbulent-viscous regime is characterized by having a Reynolds number for the bulk liquid, $Re_{flow} > 2500$ and a droplet or particle in this fluid is $Re_{drop} < 1$. To estimate the Reynolds number of a rotating mixing head the following can be used:

$$Re_{flow} = \frac{N_i D_i^2 \rho_c}{\eta_c} \quad \text{(Eq. 5)}$$

where N_i is the rotation rate per second, D_i is the diameter of the rotating part, ρ_c is the density of the continuous phase and η_c is the viscosity of the continuous phase. In this work based on the geometry of the head, the rotation rate and fluid properties the flow Reynolds number is on the order of 13000. Batch rotor–stator mixers are characterized

by a single power number, P_O, and power dissipation is calculated in the same way as for stirred tanks (Hall, Cooke, Pacek, Kowalski, & Rothman, 2011):

$$P = P_O \rho_c N_i^3 D_i^5 \quad \text{(Eq. 6)}$$

The power number depends on the type of mixer and flow regime. For turbulent flow in batch rotor–stator homogenizers, Padron (2001) measured power numbers of a variety of designs Po ∈ 1.7–3.0, and 2.1 for the mixer with the closets geometry to that of the one used in the present study. To get the power density the power is divided by the active volume of the rotor, i.e. D_i^3 giving (Doran, 1995):

$$\varepsilon = P_O \rho_c N_i^3 D_i^2 \quad \text{(Eq. 7)}$$

For the device used in our study we have estimated the energy density delivered to the fluid available for emulsification to be on the order of 10^6 W/m^3.

Turbulent flow is characterised by eddies which means that the local flow velocity, u, generally differs from the time average velocity value, $\bar{u}$, but the average difference is zero and this is characterized by the root-mean square average velocity, $u' = \langle (u - \bar{u})^2 \rangle^{1/2}$. Turbulent flow has a spectrum of eddy sizes, where the largest eddies have the highest u'. Large eddies transfer their kinetic energy to smaller ones which have a smaller $\bar{u}$ but because of their size have a larger velocity gradient, $\bar{u}/l$. This continues until the smallest eddy size is achieved and is called the Kolmogorov scale, l_o given by: $l_o = \eta_c^{3/4} \rho_c^{-1/2} \varepsilon^{-1/4}$. Local flow velocity is depending on the distance scale, x considered, and for scales comparable to the size of energy-bearing eddies, $x \approx l_e$, the velocity near that eddy is: $u'(x) = \varepsilon^{1/3} x^{1/3} \rho_c^{-1/3}$ and the velocity gradient neat that eddy is: $u'(x)/x$. If on the other hand we consider the local flow on a scale smaller than the energy bearing, $x \ll l_e$, the local flow velocity is given by: $u'(x) = \varepsilon^{1/2} x \eta_c^{-1/2}$ and thus the local velocity gradient is now independent of distance as the length scale cancels out. In the system studied in this work, ε is 10^6, making l_o 5 µm thus the stabilizing particles are smaller than the Kolmogorov scale, i.e. the smallest eddies. This means that both types of particles are following their stream line. Furthermore due to the highly anisotropic shape of the CNC (aspect ratio over 10) CNC particles are also prone to shear alignment in viscous flow (Yoshiharu, Shigenori, Masahisa, & Takeshi, 1997). Since both particles studied have a diameter less than the Kolmogorov scale we can calculate the particle Reynolds number for turbulent viscous flow regime on the length scale of the

particle, $x \approx d_p$: $Re_{pTV} = d_p^3 \varepsilon^{1/2} \rho_c \eta_c^{-3/2}$ which is for NQ on the order of 10^{-7} and for CNC 10^{-10}. Since $Re_{flow} > 2500$ and $Re_{particle} \ll 1$ we can confirm that we are well in the turbulent-viscous flow regime on the scale of the particles. For a more rigorous explanation the interested reader is directed to other works (McClements David, 2004; Walstra, 1993, 2005; Walstra & Smulders, 1998). Thus, we can use the following equation to estimate the magnitude hydrodynamic force transporting the particles towards the oil-water interface (radius R):

$$F_{a \to R(TV)} \approx a^2 \eta_c^{1/2} \varepsilon^{1/2} \quad \text{(Eq. 8)}$$

Under the homogenization conditions used, this force is approximately 10^{-11} N for NQ granules, and 10^{-13} for CNC particles. This means when the particles are experiencing a convection-dominated adsorption regime, NQ particles which are a factor 10 larger in size, experience a transport force that is a factor 100× larger than the CNC particles.

4.2 Effect of particle geometry on characteristic adsorption times

In the case of particles being transported to the oil water interface of a drop in turbulent viscous flow, the characteristic adsorption time t_A can be estimated as follows (Walstra, 2005):

$$t_A \approx \frac{\Gamma_M}{C_p 2R \sqrt{\frac{\varepsilon \rho_c}{\eta_c}}} \quad \text{(Eq. 9)}$$

For similar hydrodynamic conditions, adsorption time scales linearly with particle size (c.f. equation 4a and 4b). Thus the smaller the particles, the faster they can cover the surface at equivalent bulk concentration, assuming there is no barrier to adsorption.

4.1.3 Minimum required coverage as a function of particle size

The larger the particles and the lower the contact angle the greater the distance they will extend into the continuous aqueous phase and the question arises: How close do particles have to be to prevent coalescence by steric hindrance? Consider Fig. 5, and situation of relatively low coverage to the extent that the scarcity of particle can lead to the situation described. Given a certain drop curvature and particle radius (amount protruding into the

continuous phase) there will be a minimum distance between particles that can prevent oil-oil contact between two partially covered drops. As the concentration of particles on the oil water interface increases the spacing between them decreases (Fig 6. middle). This reduces the oil-apex height (h') and once it is less than half the protrusion height (h_w) of the particles into the water phase oil drops of radius R will be prevented from coalescing by a geometric steric hinder.

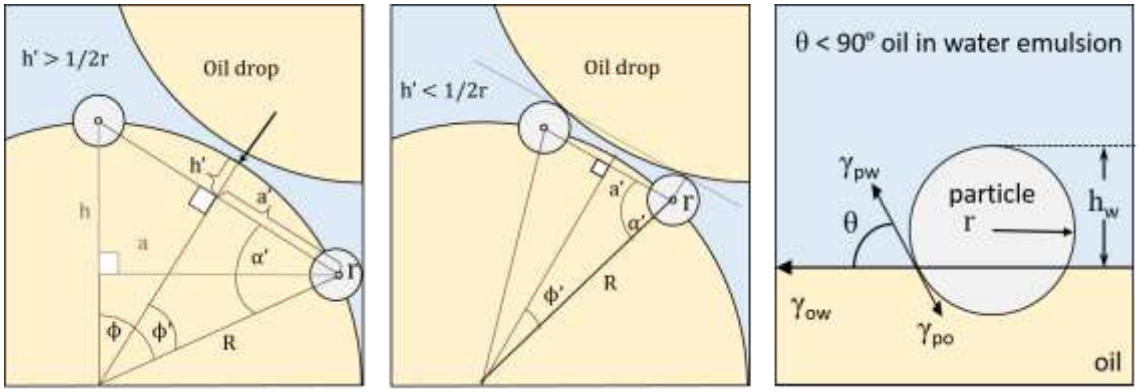

Fig. 5. Schematic illustration of minimum particle spacing required to achieve static hindrance between approaching drops. Left – not enough particles allow oil interfaces to touch, middle – distance between is small enough to prevent contact. Protrusion height h_w is determined by the contact angle Θ and the particle radius r. Note: for the top oil drop there are 2 particles as well, rotated 90 degrees out of plane to the bottom drop.

Through geometric analysis we can estimate the minimum surface coverage for particles of a given size on droplets. The particle the protrusion height (h_w) depends on its' radius r and the contact angle θ.

$$h_w = r(1 + cos\theta) \quad \text{(Eq. 10)}$$

From this we can calculate the maximum oil-apex height (h') before coalescence of droplets of radius R:

$$h' = R - \sqrt{R^2 - \frac{a^2}{4}} \quad \text{(Eq. 11)}$$

$$h'_{max} = \frac{r(1+cos\theta)}{2} \quad \text{(Eq. 12)}$$

$$a = \sqrt{h(2R - h)} \quad \text{(Eq. 13)}$$

$$h = R(1 - sin\alpha) \quad \text{(Eq. 14)}$$

$$\alpha = \frac{\pi}{2} - \phi \quad \text{(Eq. 15)}$$

From this we can then calculate the interfacial area between the particles on the surface of the droplets using the equation for a spherical section:

$$S_{sec} = \pi R(2h' + a'), \quad \text{(Eq. 16)}$$

as well as the area occupied by the particles:

$$S_p = \frac{\pi}{2} r^2. \quad \text{(Eq. 17)}$$

The surface coverage for this section is thus:

$$\varphi = \frac{S_p}{S_{sec}} \quad \text{(Eq. 18)}$$

In the case of NQ and CNC we can estimate the minimum number of particles that need to be adsorbed onto the interface to achieve this geometric minimum. For droplets of 50 µm in diameter this is equivalent to 50 to 75 individual NQ particles of 1.7 µm in diameter (depending on the contact angle) and for CNC, 600 to 850 individual particles are needed, assuming that the governing dimensions is the particle shortest length, i.e. 17 nm. This is a surprisingly small number, and should be considered as an extreme case. It is also important to consider here that there are many more CNC particles per unit volume of the continuous phase per mass. Taking the density to be 1500 kg/m^3, the number of particles for NQ and CNC per mg (particles) are 2.6×10^8 and 2.6×10^{13} respectively. On the surface of an oil drop at full coverage this is ~ 15800 mg/m^2 for NQ and 21 mg/m^2 for CNC. As a consequence, even though the interface needs 600 to 800 CNC particles to achieve steric coverage (10 times that of NQ) the availability of CNC is considerably larger per volume of continuous phase for CNC. Still the mass adsorbed at the interface at full coverage remains 100 times less for CNC.

4.1.4 Effect of particle geometry on barriers to adsorption

As particles approach the oil-water interface they may experience a barrier to adsorption arising from electrostatic repulsion. The maximum value of this interaction force scales with particle radius a when the particle is much smaller than the oil droplet radius ($a \ll R$). However the magnitude is very system dependent as it is influenced by the electrolyte concentration in the continuous phase, the nature of the particles and dispersed phase. A

more detailed discussion of this can be found elsewhere (Binks, 2002; Tcholakova et al., 2008). Another important aspect in this is not just the overall size but also the shape of the stabilizing particles. In the calculation of the repulsion force, the a term is simply radius for spherical particles, but in cases of non-spherical particles, or fractal aggregates it is the sharpest radius of curvature of the approaching mass, a_{min}. Therefore fractal aggregates of smaller particles, as well as sharp edged particles will have a much lower barrier to adsorption than smooth spherical particles with an equivalent overall size (Tcholakova et al., 2008) Fig. 6, left. In the present study, the NQ granules in the above analysis, the radius a has been across the entire granule, however in the SEM micrograph of NQ granules in Fig. 4B, they are quite polyhedral in shape with sharper edges, thus radii of curvature much smaller than 1 µm can be observed. In the case of ellipsoidal CNC, the minor axis is the sharpest radii and thus the difference between these two particles with respect to repulsive force (all else being equal) is at most a factor of 10 based on geometry alone.

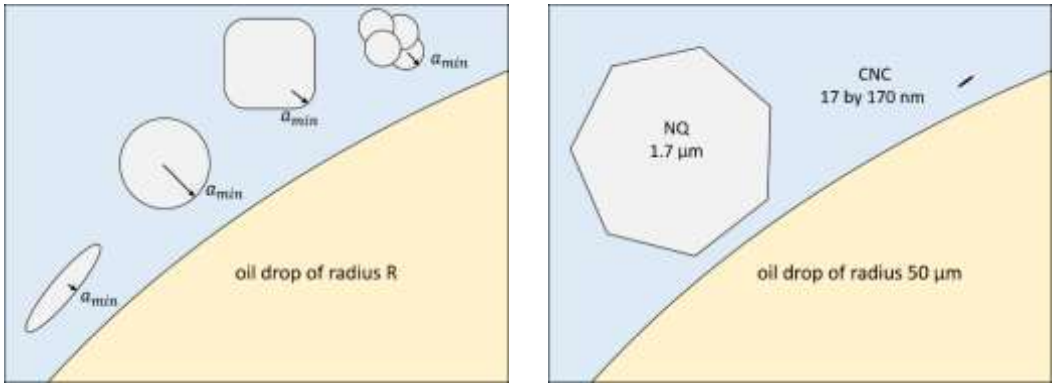

Fig. 6. Illustration of various approach radii for particles of different shapes (left). Relative sizes of NQ and CNC (right).

4.2 Particle mixture and stabilization mechanism.

4.2.1 Nature of the particles

NQ particles and CNC particles present a rather hydrophilic character, owing to the fact that they result from non-modified polysaccharide materials, which leads to the formation of oil-in-water emulsion, as the higher affinity of the particle for water promotes a higher partitioning in the water phase. The titration carried out by streaming potential showed a relatively large difference in terms of absolute charge density, around 250 µEquiv/g and 5 µEquiv/g for CNC and NQ, respectively. However, these values give an indication that

582 the surface charge density, once normalized to the specific surface of the particles is
583 comparable. CNC has, based on geometrical consideration, a specific surface area of
584 about 250 m^2/g while, the larger size of NQ particles gives a value of around 5 m^2/g, thus
585 yielding similar surface charge densities. This implies, to some extent, that their
586 wettability is comparable. Again, their tendency in forming predominantly oil-in-water
587 emulsions points in that direction.

588 Even though the particles have similar charge densities, particle-particle interaction
589 distance compared to the particles diameter is significantly different. In other words, for
590 NQ particles, the particle diameter is larger than the range of interactions of the particles,
591 while for the CNC it is about the same. This implies that the range of the electrostatic
592 repulsion between the CNC rods will be important compared to the size of the particles,
593 while most likely negligible for NQ particles. Tests carried out with and without salts for
594 NQ particles stabilized emulsions showed very little difference while the CNC-based
595 emulsions were strongly affected by the absence of salt.

596 Another hypothesis to support the predominant character of NQ particles can be related
597 to capillary action (Fig. 7 left). The question of capillary action between particles at
598 interface has been widely debated and still many uncertainties remain when it comes to
599 its effectiveness. However, the current system, by allowing competition between particle
600 of different size and shape, may provide some hints on this debated question. For the sake
601 of simplicity, as this topic does not constitute the main topic of this paper, the particles
602 will be regarded as spherical for the NQ particles, of about 1 µm in diameter and
603 cylindrical for the CNC, with a diameter of 10 nm and a length of 200 nm. Our approach
604 will be mostly qualitative, but it is important to stress the differences in size the system is
605 constituted of.

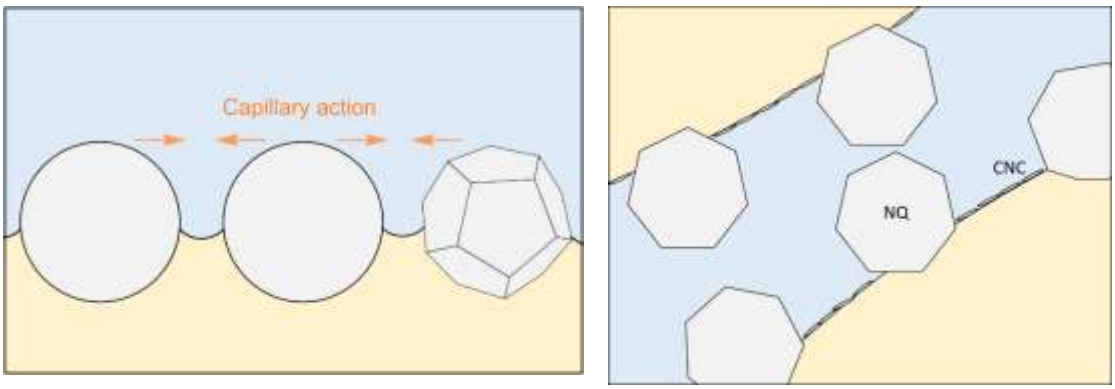

Fig. 7. Representation of the capillary action on the NQ particles positioned at an oil-water interface (left). Representation to scale of a mixed interfacial compositi.on (right).

Based on previous observations done by Kalashnikova, Bizot, Bertoncini, Cathala, and Capron (2013) the CNC particles tends to lie flat at the interface and a simple approach would be to consider the capillary action between 10 nm particle versus the forces between 1 µm sized particles. Accounting for that approximation, the CNC particles are most likely not affecting the interface as their dimensions are relatively small (Kralchevsky, Dushkin, Paunov, Denkov, & Nagayama, 1995) while microns-sized particles tend to deform the interface. The consequence is that the particles will get closer to minimize the interface deformation, thus improving the packing (McGorty, Fung, Kaz, & Manoharan, 2010). In addition the size of CNC particle in its shorter dimension is in the range of the interfacial distortion, i.e. 10 nm (Langevin, 2003).

4.2.2 Tentative explanation of the mixed systems stabilization mechanism.

As described earlier, the resulting droplet size for a given particle size and concentration assuming there is no barrier to transport or adsorption expressed as d_{32} should scale with a/C_p and can be estimated with equation 3. However in the case of NQ particles we get smaller drops than what is predicted. Several factors can explain that mostly related to particles packing and surface coverage. In the case of CNC the droplets are larger than the prediction. This is explained by the smaller particles having a smaller convective transport force which scales with a^2 that even though there is shorter characteristic time for adsorption (because there are much more CNC particles per m^3 than NQ) that relatively smaller convective transport force is not always enough to overcome the barrier to adoption which scales with the minimum curvature of the particles. Furthermore, the small CNC particles cannot benefit from further capillary action helping in the particles packing at the interface. Overall, this implies that, despite the Pickering nature of the emulsion, there are differences in the way the particles adsorb at the interface.

The competitive experiments somewhat reflect this tendency. When NQ is introduced first and an emulsion is formed, the addition of CNC in presence of further shearing does not influence the droplet size. The optical microscopy seems also to indicate the absence of CNC at the interface. However the situation is very different when stating the emulsion

on a CNC base followed by the introduction of NQ particles. This leads to mixed interfacial composition, as illustrated in Fig. 7 right. This also gave the possibility of introducing principle of mixed particles stabilized systems, proving that, for energy reasons, it is necessary to build up the system starting from the smallest particles followed by the larger sizes. Furthermore this gives new means to control the droplet size without compromising the stabilization mechanisms.

In that sense, a parallel can be drawn with the principle of electrosteric stabilization often employed in surfactant stabilized emulsions, where the dual action of ionic and non-ionic surfactants will provide two distinct features in a mixed layer at the interface, promoting stability. However, in the present case, we are not dealing with stability against coalescence induced by electrolyte concentration or temperature changes. Here, in the context of Pickering emulsions, the large particles provide a steric barrier to droplet coalescence, yet the smaller particles may play another role and their positioning at the interface will mostly affect the interfacial energy as well as the possibility of Ostwald ripening.

5. Conclusions

The results revealed that it is possible to create an emulsion with a combination of particles differing in size and shape, while very similar in terms of surface chemistry, native starch isolated from quinoa (NQ) and cellulose nanocrystals (CNC). The order of addition was found to be determinant with respect to which species prevails at the droplet interface. When CNC were added prior to the NQ, the size of the emulsion droplets was mostly governed by the CNC, and the latter could be displaced by the larger NQ. This predominance of the NQ in terms of energy of adsorption was confirmed by the fact they somewhat hindered the introduction of CNC at the interface.

We suggest that several factors can explain this behavior, and relates to the emulsification process as well as to the stabilization mechanism. First, we suggest that the large particles experience larger turbulences and shear forces during the emulsification, implying that their propensity of meeting the interface is higher. This is especially true as the large particles of this study are spherical while the small are fiber-like and prone to shear alignment. Second, because of the large difference in size of the particles compared to the droplet dimensions, the packing is affected at the oil-water interface. In a sense, particle

which size is in the same dimension as the Debye length of the medium may locally pack less well than particle significantly larger than the characteristic length. Third, the large size of NQ enables the possibility of inter-particle capillary action, which is less likely with smaller particle with sizes in the same range as the interfacial distortion. Furthermore, due to the portion of the particle protruding in the continuous phase, relatively large in comparison to the droplet diameter, we demonstrate the benefit of partly having large particles to prevent coalescence by providing a sufficient steric hindrance. Taken together, and with the higher stability observed against destabilization phenomena obtained when the Pickering emulsions were prepared with a combination of CNC particles NQ particles, we suggest that the mechanism of stabilization is actually dual. While the large particles prevent coalescence, the small particles can help regulate the curvature of the interface, and thus govern the droplet size.

The possibility of tuning the properties of emulsions by mixing particles of different size and shapes offers a different approach to rationalize the concept of particle wetting and positioning at the oil-water interface and a means to study the role of particle-particle interactions on the Pickering emulsion stability.

6. Acknowledgements

This study was supported by the Crafoord Foundation (Grant # 20150921) and the Swedish Research Foundation (Grant # 2015-03970).

7. References

Arditty, S., Whitby, C. P., Binks, B. P., Schmitt, V., & Leal-Calderon, F. (2003). Some general features of limited coalescence in solid-stabilized emulsions. *European Physical Journal E: Soft Matter Biol. Phys.*, 11(3), 273-281.

Aveyard, R., Binks, B. P., & Clint, J. H. (2003). Emulsions stabilised solely by colloidal particles. *Advances in Colloid and Interface Science*, 100, 503-546.

Binks, B. P. (2002). Particles as surfactants - Similarities and differences. *Current Opinion in Colloid and Interface Science,* 7(1-2), 21-41.

Bondeson, D., Mathew, A., & Oksman, K. (2006). Optimization of the isolation of nanocrystals from microcrystalline cellulose by acid hydrolysis. *Cellulose,* 13(2), 171-180.

Capron, I., & Cathala, B. (2013). Surfactant-Free High Internal Phase Emulsions Stabilized by Cellulose Nanocrystals. *Biomacromolecules,* 14(2), 291-296.

Cherhal, F., Cousin, F., & Capron, I. (2016). Structural Description of the Interface of Pickering Emulsions Stabilized by Cellulose Nanocrystals. *Biomacromolecules,* 17(2), 496-502.

Cunha, A. G., Mougel, J.-B., Cathala, B., Berglund, L. A., & Capron, I. (2014). Preparation of double Pickering emulsions stabilized by chemically tailored nanocelluloses. *Langmuir,* 30(31), 9327-9335.

Dhital, S., Shrestha, A. K., & Gidley, M. J. (2010). Relationship between granule size and in vitro digestibility of maize and potato starches. *Carbohydrate Polymers,* 82(2), 480-488.

Doran, P. M. (1995). *7 - Fluid Flow and Mixing*. In P. M. Doran (Ed.), *Bioprocess Engineering Principles* (pp. 129-163). London: Academic Press

Frelichowska, J., Bolzinger, M.-A., Pelletier, J., Valour, J.-P., & Chevalier, Y. (2009). Topical delivery of lipophilic drugs from o/w Pickering emulsions. *International Journal of Pharmaceutics,* 371(1–2), 56-63.

Frelichowska, J., Bolzinger, M. A., Pelletier, J., Valour, J. P., & Chevalier, Y. (2014). *Skin Penetration from Pickering Emulsions*. In *Advances in Dermatological Sciences* (pp. 124-142): The Royal Society of Chemistry

Habibi, Y., Lucia, L. A., & Rojas, O. J. (2010). Cellulose Nanocrystals: Chemistry, Self-Assembly, and Applications. *Chemical Reviews,* 110(6), 3479-3500.

Hall, S., Cooke, M., Pacek, A. W., Kowalski, A. J., & Rothman, D. (2011). Scaling up of silverson rotor–stator mixers. *The Canadian Journal of Chemical Engineering,* 89(5), 1040-1050.

Kalashnikova, I., Bizot, H., Bertoncini, P., Cathala, B., & Capron, I. (2013). Cellulosic nanorods of various aspect ratios for oil in water Pickering emulsions. *Soft Matter*, 9(3), 952-959.

Kralchevsky, P. A., Dushkin, C. D., Paunov, V. N., Denkov, N. D., & Nagayama, K. (1995). *Lateral capillary forces between colloidal particles incorporated in liquid*

734 *films or lipid bilayers*. In J. Appell & G. Porte (Eds.), *Trends in Colloid and*
735 *Interface Science IX* (pp. 12-17). Darmstadt: Steinkopff
736 Langevin, D. (2003). Electric-Field-Induced Capillary Attraction between Like-Charged
737 Particles at Liquid Interfaces. *ChemPhysChem*, 4(10), 1057-1058.
738 Marefati, A., Bertrand, M., Sjöö, M., Dejmek, P., & Rayner, M. (2016). Storage and
739 digestion stability of encapsulated curcumin in emulsions based on starch granule
740 Pickering stabilization. *Food Hydrocolloids*.
741 Marefati, A., Rayner, M., Timgren, A., Dejmek, P., & Sjöö, M. (2013). Freezing and
742 freeze-drying of Pickering emulsions stabilized by starch granules. *Colloids and*
743 *Surfaces A: Physicochemical and Engineering Aspects*, 436, 512-520.
744 Marefati, A., Sjöö, M., Timgren, A., Dejmek, P., & Rayner, M. (2015). Fabrication of
745 encapsulated oil powders from starch granule stabilized W/O/W Pickering
746 emulsions by freeze-drying. *Food Hydrocolloids*, 51, 261-271.
747 Marku, D., Wahlgren, M., Rayner, M., Sjöö, M., & Timgren, A. (2012). Characterization
748 of starch Pickering emulsions for potential applications in topical formulations.
749 *International Journal of Pharmaceutics*, 428(1), 1-7.
750 Matos, M., Gutiérrez, G., Iglesias, O., Coca, J., & Pazos, C. (2015). Enhancing
751 encapsulation efficiency of food-grade double emulsions containing resveratrol or
752 vitamin B 12 by membrane emulsification. *Journal of Food Engineering*, 166,
753 212-220.
754 Matos, M., Lobo, A., Benito, J. M., Coca, J., & Pazos, C. (2012). Extending the useful
755 life of metalworking fluids in a copper wire drawing industry by monitoring their
756 functional properties. *Tribology Transactions*, 55(5), 685-692.
757 Matos, M., Marefati, A., Gutiérrez, G., Wahlgren, M., & Rayner, M. (2016). Comparative
758 Emulsifying Properties of Octenyl Succinic Anhydride (OSA)-Modified Starch:
759 Granular Form vs Dissolved State. *PloS one*, 11(8), e0160140.
760 Matos, M., Timgren, A., Sjöö, M., Dejmek, P., & Rayner, M. (2013). Preparation and
761 encapsulation properties of double Pickering emulsions stabilized by quinoa
762 starch granules. *Colloids and Surfaces A: Physicochemical and Engineering*
763 *Aspects*, 423, 147-153.
764 McClements David, J. (2004). *Emulsion formation*. In *Food Emulsions*: CRC Press
765 McGorty, R., Fung, J., Kaz, D., & Manoharan, V. N. (2010). Colloidal self-assembly at
766 an interface. *Materials Today*, 13(6), 34-42.

Mikulcová, V., Bordes, R., & Kašpárková, V. (2016). On the preparation and antibacterial activity of emulsions stabilized with nanocellulose particles. *Food Hydrocolloids*, 61, 780-792.

Padron, G. A. (2001). Measurement and comparison of power draw in batch rotor-stator mixers. *University of Maryland, College Park, MD, USA*.

Pickering, S. U. (1907). CXCVI.—emulsions. *Journal of the Chemical Society, Transactions*, 91, 2001-2021.

Ramsden, W. (1903). Separation of Solids in the Surface-Layers of Solutions and'Suspensions'(Observations on Surface-Membranes, Bubbles, Emulsions, and Mechanical Coagulation).--Preliminary Account. *Proceedings of the Royal Society of London*, 72, 156-164.

Rayner, M., Sjöö, M., Timgren, A., & Dejmek, P. (2012). Quinoa starch granules as stabilizing particles for production of Pickering emulsions. *Faraday Discussions*, 158(1), 139-155.

Rayner, M., Timgren, A., Sjöö, M., & Dejmek, P. (2012). Quinoa starch granules: a candidate for stabilising food-grade Pickering emulsions. *Journal of the Science of Food and Agriculture*, 92(9), 1841-1847.

Tcholakova, S., Denkov, N. D., & Lips, A. (2008). Comparison of solid particles, globular proteins and surfactants as emulsifiers. *Physical Chemistry Chemical Physics*, 10(12), 1608-1627.

Timgren, A., Rayner, M., Sjöö, M., & Dejmek, P. (2011). Starch particles for food based Pickering emulsions. *Procedia Food Science*, 1, 95-103.

Walstra, P. (1993). Principles of emulsion formation. *Chemical Engineering Science*, 48(2), 333-349.

Walstra, P. (2005). *8 Emulsions*. In J. Lyklema (Ed.), *Fundamentals of Interface and Colloid Science* (pp. 1-94): Academic Press

Walstra, P., & Smulders, P. E. A. (1998). *Chapter 2 Emulsion Formation*. In *Modern Aspects of Emulsion Science* (pp. 56-99): The Royal Society of Chemistry

Welss, T., Basketter, D. A., & Schröder, K. R. (2004). In vitro skin irritation: facts and future. State of the art review of mechanisms and models. *Toxicology in vitro*, 18(3), 231-243.

Yoshiharu, N., Shigenori, K., Masahisa, W., & Takeshi, O. (1997). Cellulose Microcrystal Film of High Uniaxial Orientation. *Macromolecules*, 30(20), 6395-6397.

Zoppe, J. O., Venditti, R. A., & Rojas, O. J. (2012). Pickering emulsions stabilized by cellulose nanocrystals grafted with thermo-responsive polymer brushes. *Journal of colloid and interface science*, 369(1), 202-209.